

# Sample geometry and the brittle-ductile behavior of edge cracks in 3D atomistic simulations by molecular dynamics

V. Pelikán, P. Hora, A. Machová, R. Kolman, A. Uhnáková

Institute of Thermomechanics AS CR, v. v. i.  
Prague, Czech Republic



8th MSMF / June 27-29, 2016 / Brno, Czech Republic

# Introduction

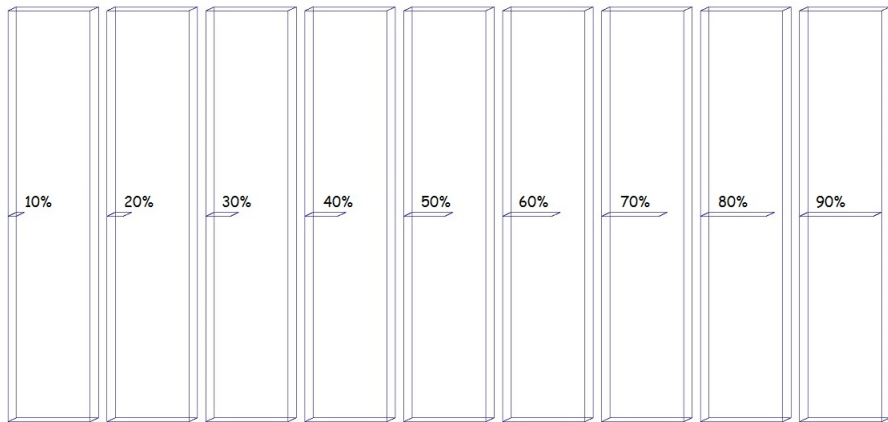
Crack (001)[010] (crack plane/crack front) under monotonic uniaxial tension can produce dislocations in 3D bcc iron crystals in the available inclined slip systems  $\langle 111 \rangle \{101\}$ , while the crack  $(\bar{1}10)[110]$  can emit dislocations in the inclined slip systems  $\langle 111 \rangle \{112\}$ , both under monotonic tension or cyclic loading in mode I. It occurs at low temperature but also at room temperature as experiments on iron crystals confirmed. However, ductile behavior at the crack front depends not only on the stress intensity  $K_I$  but also on so-called T-stress acting parallel to crack plane. Our previous molecular dynamic (MD) simulations with central cracks have been shown that the sign of T-stress influences their brittle-ductile behavior under loading in mode I. Negative T-stress supports dislocation emission or twin generation at the crack tip, while positive T-stress may lead to cleavage fracture. It can be easily understood by Rice prediction for inclined slip systems:  $\tau_{crit} = \tau_{crit}^0 + T \sin(\alpha) \cos(\alpha)$ , where  $\tau_{crit}$  is the stress barrier for the slip process and  $\alpha$  is the inclination angle of the slip system with respect to the axis of potential crack extension. Here we present new MD results focused to 3D bcc iron crystals with short edge cracks (negative T-value) and longer cracks with positive T-stress according to static predictions for isotropic continuum by Fett.

# MD simulations in 3D crystals of bcc iron

We consider a pre-existing edge crack of the length  $a$  placed in the middle of a rectangular sample of the length  $L$ , width  $W$  and thickness  $B$ . Edge cracks with orientation  $(\bar{1}10)[110]$  and  $(001)[010]$  are studied in atomistic samples with the geometries  $a/W$ ,  $L/W$  and  $B/W$  accessible for fracture experiments. The samples are loaded by monotonic uni-axial tension (mode I) via external forces distributed in several surface layers in  $L$  direction. Surface relaxation has been performed before loading to avoid its influence on crack tip processes. The same N-body potentials for bcc iron have been used in this study as in our previous work. Newtonian equations of motion for individual atoms were solved by a central difference method using time integration step  $h = 0.01$  ps.

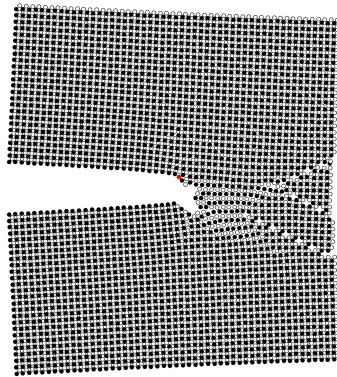
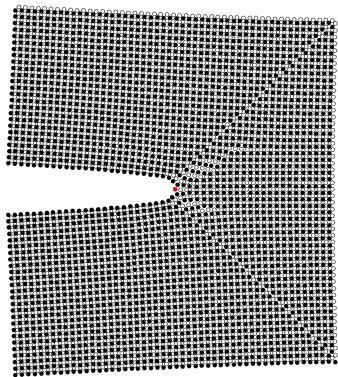
Edge crack (001)[010] was created by removing 1 layer of atoms in the direction  $W$  of potential crack extension. Number of atomic layers (001) in  $L$ -direction is 4 999, in  $W$ -direction it is 1 001, and along the crack front (in  $B$ -direction) it is 201. Total number of atoms in the perfect 3D cubic crystal corresponds to  $N_{\text{POIN}} = 252\,702\,000$  and parallel processing in MPI was used in this case. At initial temperature of 0 K, systematic studies with different ratios  $a/W = 0.1, \dots, 0.9$  have been performed with loading rate where critical Griffith stress intensity  $K_G$  was reached during 15 000  $h$ . At temperature of 300 K, the ratios  $a/W = 0.2, \dots, 0.8$  were treated. Beside free 3D simulations, periodic boundary conditions along crack front were also tested with the crack (001)[010].

# Samples

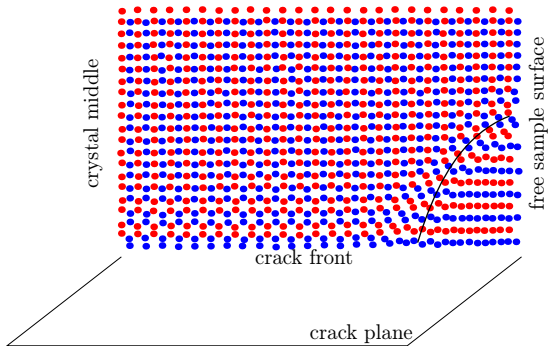


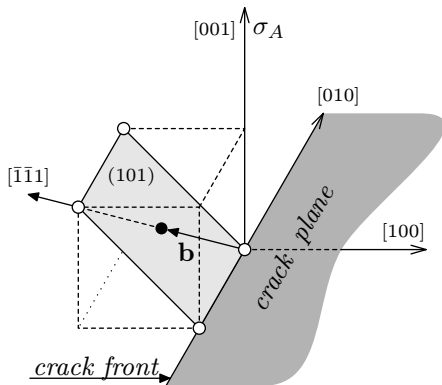
Crack length  $a/W = 0.3$ , temperature 0 K:

- a) dislocation patterns from  $\langle \bar{1}\bar{1}1 \rangle \{101\}$  slip systems on the first two surfaces layers (001), time step 17800,  $\sigma_A(t) = 2.583$  GPa;
- b) crack growth in the middle of the crystal, empty patterns come from oblique slip systems  $\langle \bar{1}\bar{1}1 \rangle \{112\}$ , time step 18 400,  $\sigma_A(t) = 2.670$  GPa.  
(The red point denotes the original crack tip atom.)



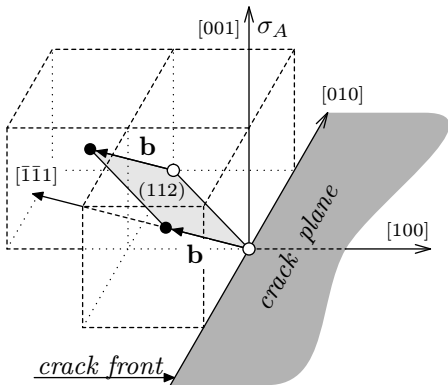
Beginning of plastic deformation:  
slip patterns on two {101} planes,  
view (101)[101]





The slip system  $(101)[\bar{1}\bar{1}1]$  is inclined to the crack plane and contains the crack front. Dislocation emission in this slip system causes crack tip blunting.

$$\tau_{disl} = 14.5 \text{ GPa.}$$

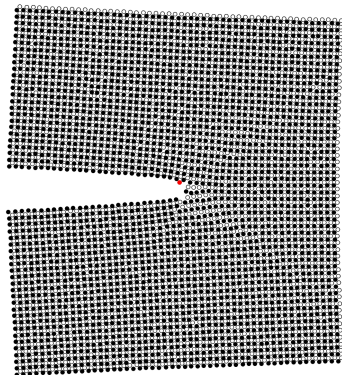
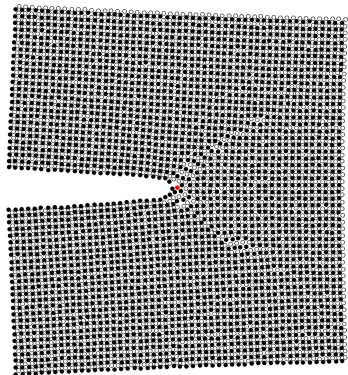


The second slip system  $(112)[\bar{1}\bar{1}\bar{1}]$  is oblique to the crack front and dislocation emission makes a jog in the crack front in the direction of  $b$ . It enables a slow plastic crack growth.  $\tau_{disl} = 16.3 \text{ GPa}$ .

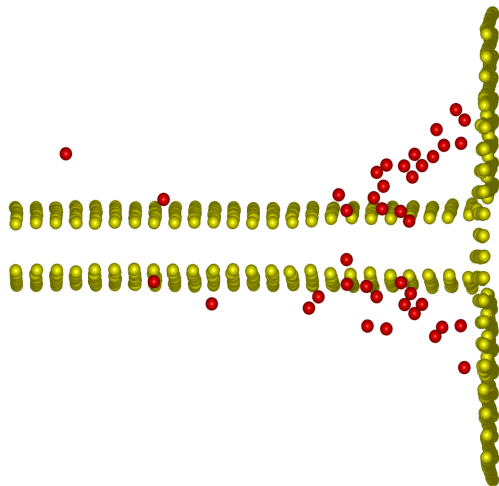
Edge crack  $a/W = 0.8$ , 300 K:

a) dislocation emission  $\langle \bar{1}\bar{1}1 \rangle \{101\}$  at free sample surfaces (001), time step 23 500,  $\sigma_A(t) = 0.965$  GPa;

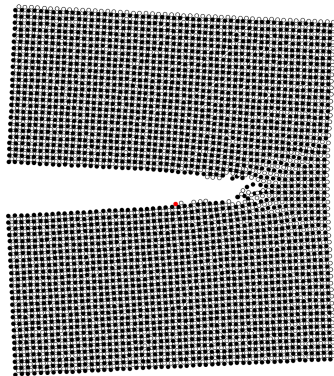
b) crack initiation in the middle, time step 25000,  $\sigma_A(t) = 1.027$  GPa.



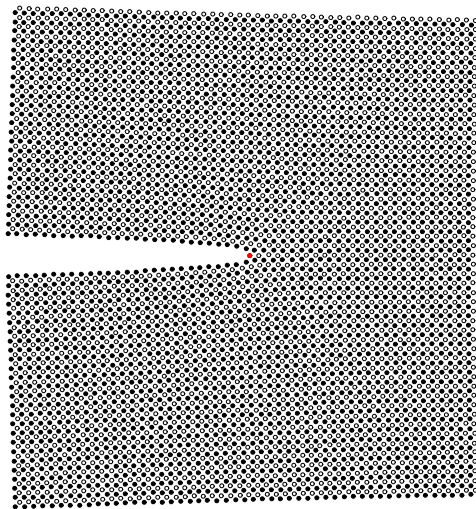
3D visualization of dislocation emission (red atoms) from the corners where the crack (yellow) penetrates free sample surface (yellow atoms).



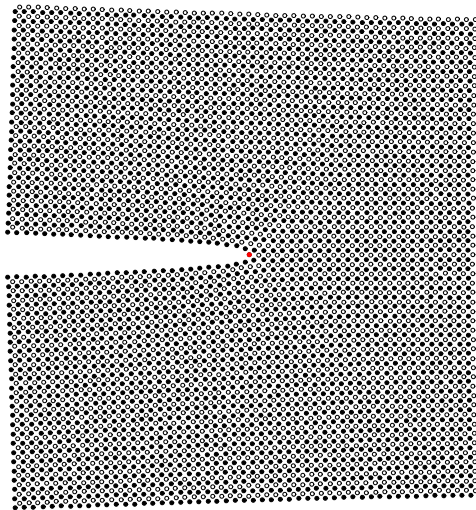
Brittle crack growth in the middle of the crystal with periodic boundary conditions along crack front,  $a/W = 0.2$ , 300 K, time step 20 000,  $\sigma_A(t) = 3.004$  GPa.



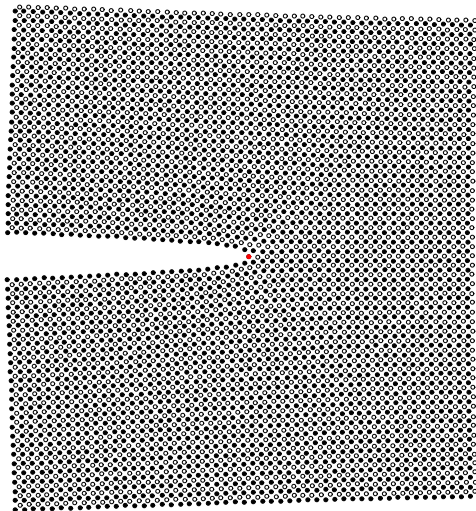
Crack growth on the surface of the crystal with periodic boundary conditions along crack front,  $a/W = 0.2$ , 300 K, time step 15 600.



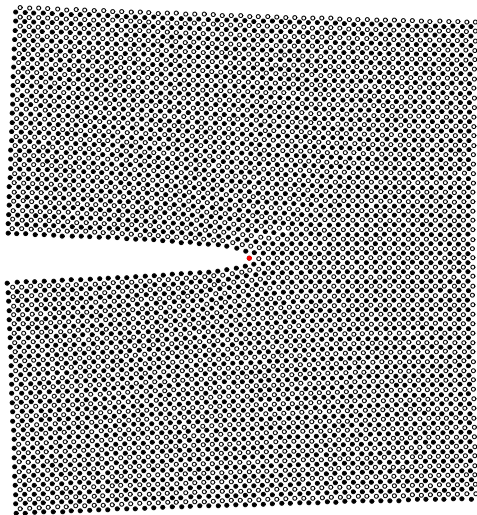
Crack growth on the surface of the crystal with periodic boundary conditions along crack front,  $a/W = 0.2$ , 300 K, time step 16 000.



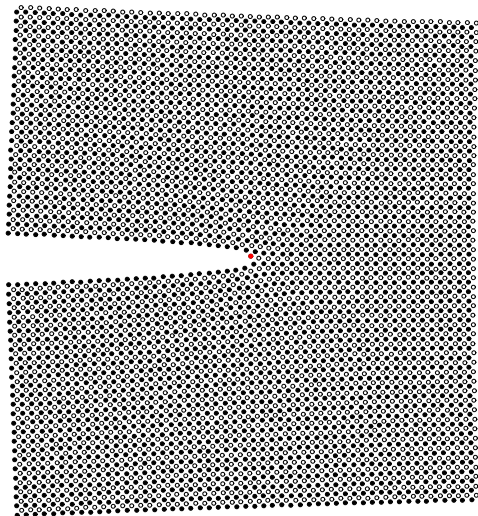
Crack growth on the surface of the crystal with periodic boundary conditions along crack front,  $a/W = 0.2$ , 300 K, time step 16 400.



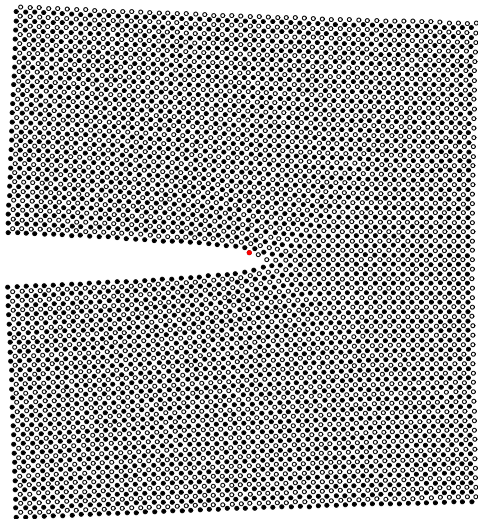
Crack growth on the surface of the crystal with periodic boundary conditions along crack front,  $a/W = 0.2$ , 300 K, time step 16 800.



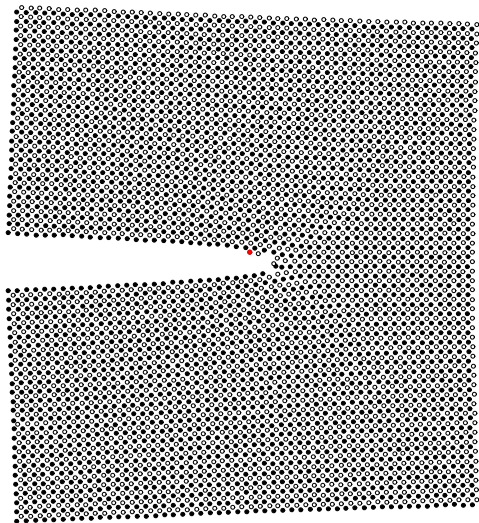
Crack growth on the surface of the crystal with periodic boundary conditions along crack front,  $a/W = 0.2$ , 300 K, time step 17 200.



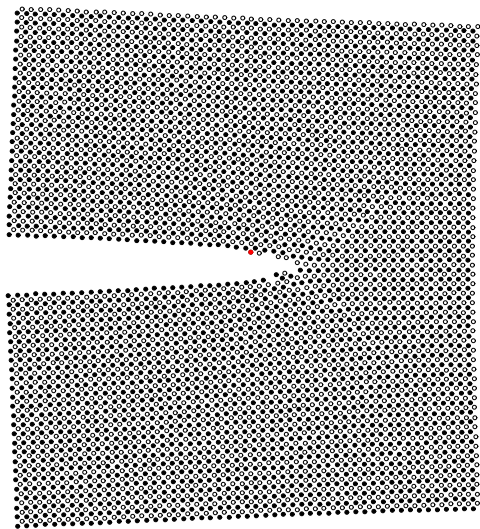
Crack growth on the surface of the crystal with periodic boundary conditions along crack front,  $a/W = 0.2$ , 300 K, time step 17 600.



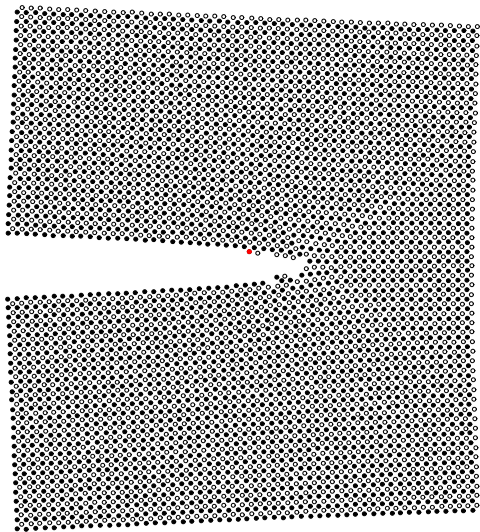
Crack growth on the surface of the crystal with periodic boundary conditions along crack front,  $a/W = 0.2$ , 300 K, time step 18 000.



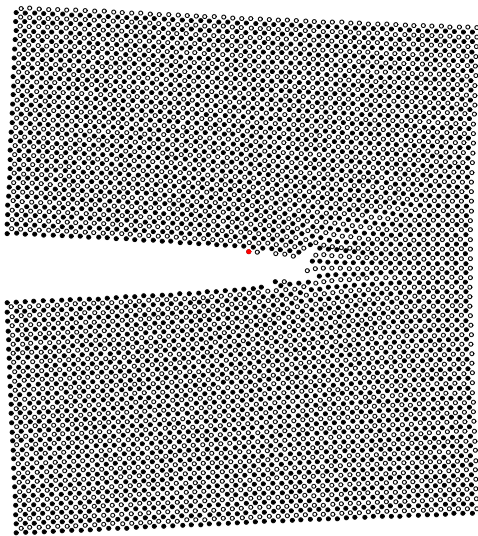
Crack growth on the surface of the crystal with periodic boundary conditions along crack front,  $a/W = 0.2$ , 300 K, time step 18 400.



Crack growth on the surface of the crystal with periodic boundary conditions along crack front,  $a/W = 0.2$ , 300 K, time step 18 800.

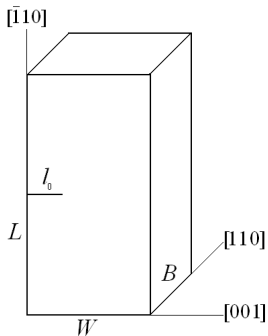


Crack growth on the surface of the crystal with periodic boundary conditions along crack front,  $a/W = 0.2$ , 300 K, time step 19 200.

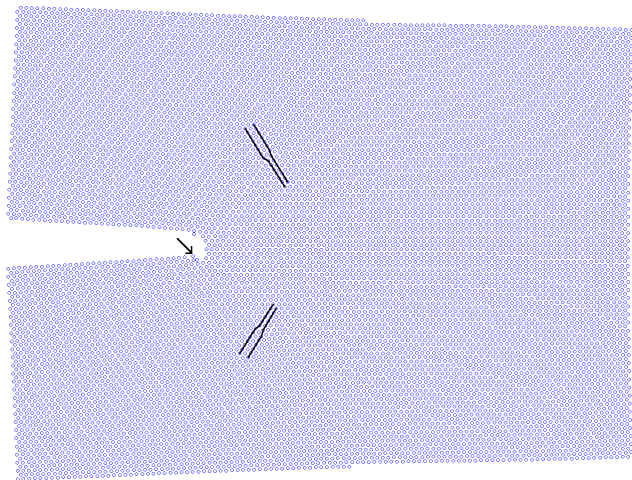


Edge crack  $(\bar{1}10)[110]$  was created by cutting interatomic bonds across the initial crack plane. Two different geometries with  $a/W = 0.3$  and  $a/W = 0.8$  have been studied with negative and positive T-stress by Fett. Initial temperature was 0 K and further thermal atomic motion was not controlled. Atomistic sample consists of 440 atomic planes  $(\bar{1}10)$  in  $L$ -direction, 220 planes  $(001)$  in  $W$ -direction and 30 planes  $(110)$  in  $B$ -direction along the crack front. Total number of atoms in the 3D crystal is  $N_{\text{POIN}} = 1\,452\,000$  and sequence processing was used to integrate Newtonian equations of motion with the same time step  $h = 0.01$  ps as above. Loading rate corresponded to  $K_G$  per 4 000  $h$ .

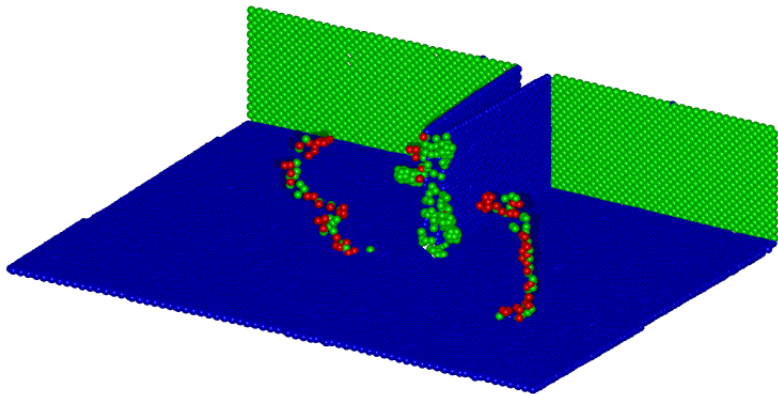
Sample geometry for crack orientation  $(\bar{1}10)[110]$  (crack plane / crack front), crack length  $a = l_0$ .



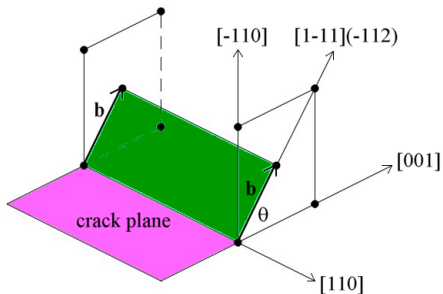
Dislocation emission on inclined slip systems  $\langle 111 \rangle \{112\}$  from the edge crack  $(\bar{1}10)[110]$  with the ratio  $a/W = 0.3$ , middle of the crystal, 0 K, time step 5 000,  $\sigma_A(t) = 5.625$  GPa, the arrow denotes the original crack tip point.



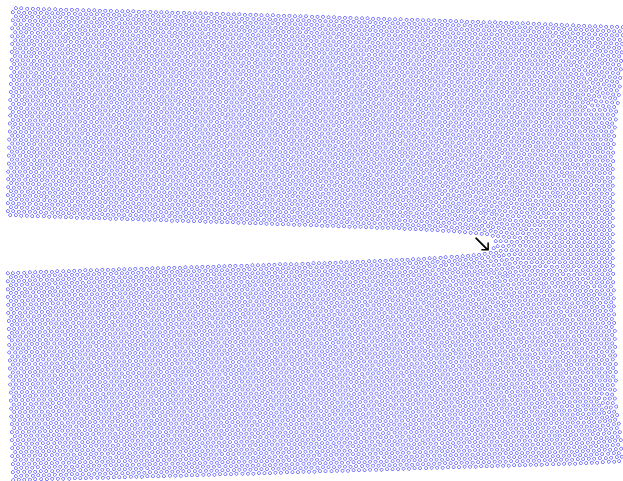
3D visualization of dislocation emission by means of coordination numbers (KNT) - see the red (KNT= 16, 17) and green (KNT = 13) atoms in front of the crack.



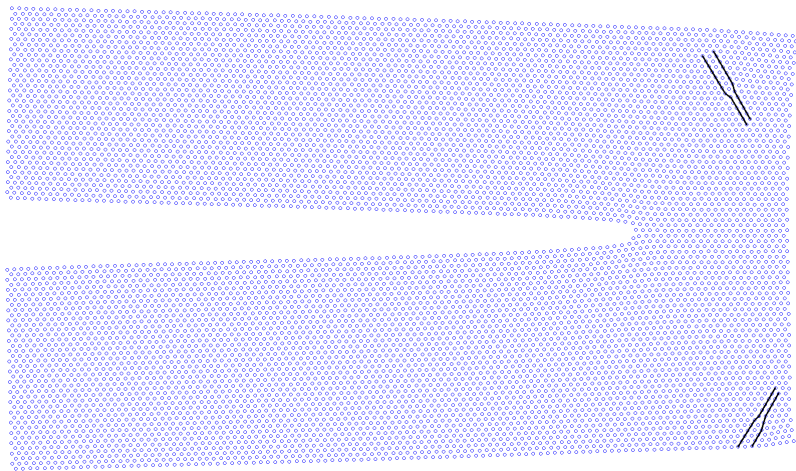
Scheme of the crack plane and inclined slip system  $\langle 111 \rangle \{112\}$  with Burgers vector  $\mathbf{b}$ .



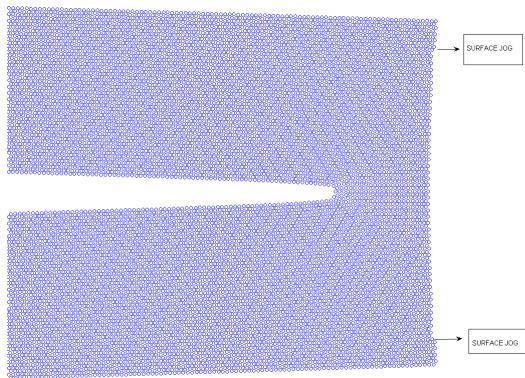
Complete edge crack  $(\bar{1}10)[110]$  with  $a/W = 0.8$  in elastic region of loading at 0 K, time step 2500.



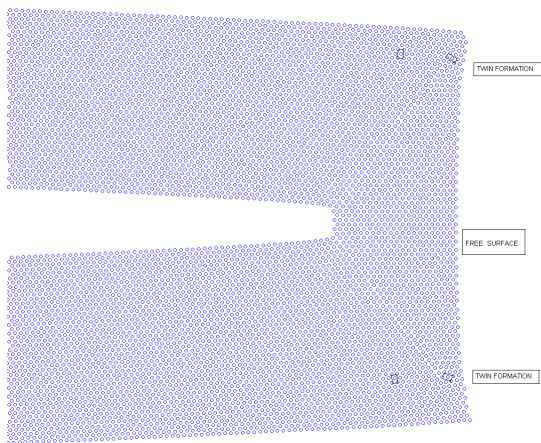
Detail from the emission of the blunting dislocations  $[1\bar{1}1](\bar{1}12)$  under angle  $55^\circ$  on surface plane (110),  $a/W = 0.8$ , 0 K, time step 3 000,  $\sigma_A(t) = 3.375$  GPa (the critical shear stress for dislocation emission with the used potential is  $\tau_{disl} = 16.3$  GPa).



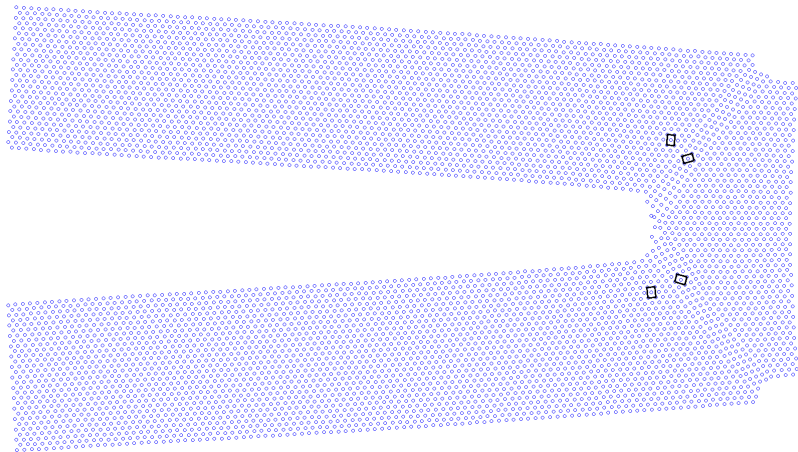
Jogs on the right free surface after arrival of the blunting dislocations from the crack front to the free surface (anti-twinning direction),  $a/W = 0.8$ , time step 3 050, new stress concentrators.



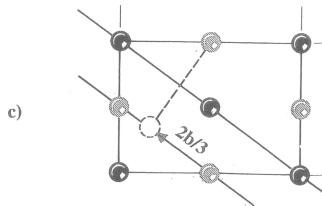
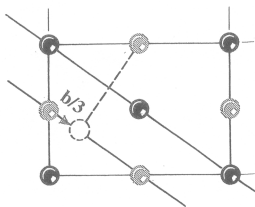
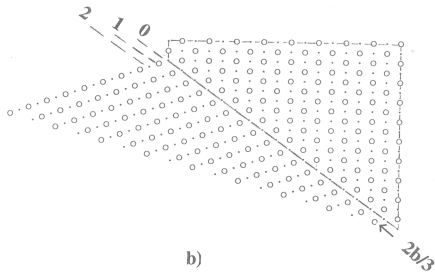
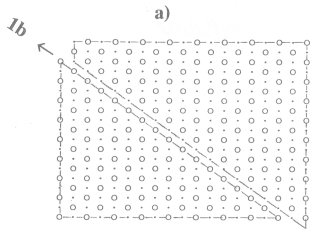
Twin formation at the right free surface,  $a/W = 0.8$ , time step 3 500. For the used potential, the stress barrier for twin formation in the easy twinning direction is  $\tau_{twin} = 9.3$  GPa, while in the hard anti-twinning direction it is 27.9 GPa.



Twin extension in the easy twinning direction from the right free surface toward the crack front, time step 4 000,  $\sigma_A(t) = 4.5$  GPa, a detail in middle of the crystal, temperature 0 K,  $a/W = 0.8$ .



Scheme for anti-twinning direction: a) dislocation formation, b) anti-twin, c) easy twinning direction ( $b/3$ ) and hard anti-twinning direction ( $2b/3$ ).



# Question time

The work was supported by the pilot project IT ASCR No. 904168 with Institutional support RVO: 61388998. The work of A. Machová was also supported by the project of the Czech Science Foundation GACR 15-20666S.